Int J Ind Chem (2017) 8:273–283
DOI 10.1007/s40090-016-0107-7

RESEARCH

Influence of synthesized nano-ZnO on cure and physico-mechanical properties of SBR/BR blends

Madhuchhanda Maiti[1] · Ganesh C. Basak[1] · Vivek K. Srivastava[1] · Raksh Vir Jasra[1]

Received: 6 June 2016 / Accepted: 7 November 2016 / Published online: 17 November 2016

Abstract This study focuses on the synthesis of zinc oxide (ZnO) nanoparticles by high temperature calcination as well as low-temperature hydrolysis methods and their efficiency as cure activator in styrene-butadiene rubber/polybutadiene rubber blend. The synthesized nano-ZnO samples were characterized by means of X-ray diffraction, BET surface area and transmission electron microscopy. The synthesized nano-ZnO samples had wurtzite structure and average particle size in the 'nm' range. ZnO nanoparticles, synthesized on sepiolite template, were of smallest particle size (maximum number of particles in the range of 7–12 nm) and highest surface area (104 m^2g^{-1}). Polyethylene glycol (PEG)-6000 coated ZnO nanoparticles had rod-like structure; average diameter of the rods was 50 nm. In the case of PEG-coated ZnO containing compounds, optimum cure time of the blend was decreased by 5 min compared to that of standard rubber grade-ZnO containing compound (used as reference). Optimum cure time was lowered by 7–10 min in the case of synthesized nano-ZnO containing compounds compared to the reference ZnO based compound in presence of conventional filler, carbon black. It was also observed from ICP-OES analysis that the presence of very little amount of magnesium in one of the synthesized ZnO has noticeable impact on cure properties. PEG-coated ZnO increased the tensile strength of gum vulcanizates by 28% compared to the reference ZnO, acting as nanofiller at 3 phr loading. The study of curing behavior in dynamic condition was carried out using DSC. The results differ slightly from static curing except PEG modified nano-ZnO. Use of ZnO nanoparticles could provide faster crosslinking, better reinforcement at lower concentration compared to reference ZnO.

Keywords Nano-ZnO · SBR · BR · Curing · Cure properties

Introduction

The rubber industries, specifically tire industries, contribute significantly to economy of a nation where automobile industry is growing at a very fast pace. Improvement in quality and safety of rubber products can have significant impact on this industry [1, 2]. Zinc oxide (ZnO) is primarily used as an activator for sulfur vulcanization of rubbers. Besides, inclusion of ZnO in the rubber compound brings other benefits viz., reduction in heat build-up, improvement of abrasion resistance and heat resistance of the vulcanizates. Furthermore, its high thermal conductivity helps to dissipate local heat concentrations in rubber products. Zinc oxide is a necessary ingredient in rubber compounds for bonding rubber to reinforcing steel cord, etc. Besides improving the properties of vulcanized rubbers, ZnO also assists in the processing of uncured rubbers. ZnO is added to rubber formulation to reduce shrinkage of molded rubber products and maintain the cleanliness of molds [3].

The road transport emission of zinc due to tire wear is the main sources of zinc pollution after iron and steel production and non-ferrous metals manufacture. This arises from the zinc content (1 wt%) of the tire-tread material [4, 5]. But some adverse environmental effects of zinc exposure have been reported. In view of the upcoming legislation and eco-labeling requirements for tires, it can be

✉ Ganesh C. Basak
ganesh.basak@ril.com

[1] Reliance Technology Group, Vadodara Manufacturing Division, Reliance Industries Ltd., Vadodara, Gujarat 391346, India

stated that it is desirable to keep the ZnO content in rubber compounds as low as possible.

In rubber industry, various kinds of vulcanization activators like CaO, MgO, CdO, CuO, PbO and NiO have been used in order replace conventional ZnO due to its toxic and fouling characteristics for aquatic flora and fauna. Although among the various activators studied, MgO shows most promising candidate in terms of activating properties in comparison to ZnO but maximum crosslinking can be achieved in the presence of ZnO only [6]. Moreover, few reports are also available that describe the effect of layered double hydroxide (LDH) on elastomeric materials in the place of ZnO. According to the literature reports, LDH material can be used as an alternative cure activator in place of ZnO and stearic acid combo in the conventional cure package for the preparation of rubber composites, and simultaneously can provide a strong platform for reduction of ZnO level in elastomer vulcanizate system [7].

In another approach, the concentration of ZnO can be minimized if the efficiency of ZnO during vulcanization can be enhanced by the maximization of the contact between the ZnO particles and the accelerators in the compound. This contact is dependent on the size, shape, specific surface area and dispersibility of the ZnO particles. Nano-sized ZnO particles have been paid more attention for their unique properties, even though there are limited open literatures available on nano-ZnO as cure activators. ZnO nanoparticles were studied as a cure activator and curing agent in natural rubber (NR), nitrile rubber (NBR), carboxylated nitrile rubber (XNBR) and chloroprene rubber (CR) by Bhowmick and his coworkers [8–10]. Similarly, it was used as cure activator in NR and CR by Joseph et al. [11, 12]. Nanostructured zinc oxide was used in crosslinking of hydrogenated butadiene-acrylonitrile elastomer and XNBR by Przybyszewska and Zaborski [13–15]. Guzman et al. synthesized mixed metal oxide nanoparticles of zinc and magnesium to reduce the ZnO levels in rubber compounds [16]. Heideman et al. studied the influence of nano-ZnO on the cure properties of solution styrene-butadiene rubber (SBR) and ethylene–propylene–diene rubber [17]. Kim et al. investigated the effect of nano-ZnO on the cure characteristics and mechanical properties of the silica-filled natural rubber/butadiene rubber compounds [18]. Jincheng and Yuehui studied the application of nano-ZnO master-batch in SBR [19].

In our previous work, we have studied the effect of nano-ZnO on the cure properties of polybutadiene rubber (BR) [20]. It was observed that the nano-ZnO reduces curing time and also enhances physico-mechanical as well thermal stability properties of butadiene rubber compound at lower concentration compared to the conventional micro-ZnO. However, to the best of our knowledge, the effect of nano-ZnO as cure activator has not yet been explored for SBR/BR rubber blend. In the open literature, it has already been reported that nano-zinc oxides are effective activators and reinforcing agents in rubber systems. The "little size effect," "surface effect" and "quantum effect" of nano-ZnO governs the properties of the composites [21]. Although considerable amount of work has been done so far on the use of nano-ZnO in place of conventional ZnO as a cure activator and for enhancing the mechanical properties of elastomer, the study on SBR/BR-nano-ZnO composites is scarcely available in the literature [22]. In the tire industry, SBR/BR blend is of considerable importance as it is widely used in passenger car tire-tread compound. Hence, investigation of nanocomposite based on SBR/BR blends and nano-ZnO would not only be providing valuable information but also have wide applications. Typically SBR/BR blend shows slower curing rate than other general purpose rubbers such as NR and BR [3]. Hence, it will be of interest to study the cure properties of this blend with nano-ZnO.

In this work, we have studied the influence of morphology, specific surface area and dispersibility of ZnO nanoparticles on the static and dynamic vulcanization of SBR/BR blends. We have studied the effect of sepiolite template and 'eco-friendly' metal oxide, magnesium oxide (MgO) on nano-ZnO in the crosslinking of the rubber blend. The influence of nano-ZnO on the properties of SBR/BR vulcanizates in the absence as well as in the presence of conventional filler was also evaluated.

Experimental

Materials

Zinc nitrate [$Zn(NO_3)_2{\cdot}6H_2O$] [molecular weight (M.W.) 297.48, 98% purity], ammonium carbonate [$(NH_4)_2CO_3$] (M.W. 157.13, 31% purity), acetone (M.W. 58.08, 99.5% purity), methanol (M.W. 32.04, 99.5% purity), sodium hydroxide pellets (M.W. 40.00, 98% purity), 1-octanol (M.W. 130.23, 99% purity), Stearic acid (M.W. 284.48, 98% purity), sulfur powder (M.W. 32.06, 99% purity), *N*-cyclohexyl-2-benzothiazole sulfenamide (CBS) (M.W. 264.42, 97% purity), microcrystalline wax, magnesium oxide (MgO) were procured from Labort Fine Chem. Pvt. Ltd., India. Standard rubber grade zinc oxide (ZnO), used as reference (designated as SZ), was supplied by Labort Fine Chem. Pvt. Ltd., India. Polyethylene glycol-6000 (PEG) was obtained from Alfa Biochem, Greece. Zinc acetate dihydrate [$Zn(CH_3COO)_2{\cdot}2H_2O$] (M.W. 219.50, 98.5% purity) and Oxalic acid (M.W. 126.07, 99.8% purity) were procured from S. D. Fine Chem. Ltd., India. *N*-(1,3-dimethyl butyl)-*N*′-phenyl-*p*-phenylenediamine (6PPD) was obtained from John Baker Inc., USA. Polybutadiene rubber (BR; Cisamer 01; ML_{1+4} at 100 °C = 45; *cis*-content 96%) was collected from

Reliance Industries Ltd., India. Styrene-butadiene rubber (SBR 1502; ML_{1+4} at 100 °C = 48) was supplied by Japan Synthetic Rubber, Japan. Sepiolite (Pangel S9) was generously supplied by Tolsa, Spain. Carbon black (N330) was procured from Philips Carbon Black Ltd., India.

Preparation of nano-ZnO

Nano-ZnO was synthesized by high temperature calcination as well as low-temperature hydrolysis methods. The typical procedures are described below.

Method-1 [9]

$Zn(NO_3)_2{\cdot}6H_2O$ and ammonium carbonate $(NH_4)_2CO_3$ were, respectively, dissolved in distilled water at a concentration of 1.0 M. Zinc nitrate solution was then slowly dropped into the vigorously stirred $(NH_4)_2CO_3$ solution with molar ratio of 2:1 to prepare the precursor. A white precipitate occurred immediately on mixing of the two solutions. Stirring was done for 3 h to have complete precipitation. The white precipitate thus obtained was filtered and repeatedly washed with distilled water to remove impurities and dried at 105 °C for 6 h. Calcination of the dried sample was carried out at 450 °C in a muffle furnace. The sample thus obtained is designated as Z1.

Method-2 [23]

0.1 M aqueous solution of oxalic acid was added to 0.1 M aqueous solution of $Zn(CH_3COO)_2{\cdot}2H_2O$ and the solution was stirred for 4 h. The white precipitates thus obtained were filtered and washed with acetone and distilled water to remove impurities and dried at 120 °C for 6 h. The dried sample was calcined at 450 °C in a muffle furnace to remove CO and CO_2 from the compound. The sample is designated as Z2.

Method- 3 [24]

The solution of Zn $(CH_3COO)_2{\cdot}2H_2O$ (0.1 M) was prepared in 50 ml methanol under stirring. 25 ml of NaOH (0.3 M) solution, prepared in methanol, was mixed with above solution under continuous stirring to get the pH of reactants between 8 and 11. These solutions were transferred into a Teflon lined sealed stainless steel autoclave and maintained at 150 °C for 12 h under autogenous pressure. It was then allowed to cool naturally to room temperature. After the reaction was complete, the resulting white solid product was washed with methanol, filtered and then dried in a laboratory oven at 100 °C. The sample is designated as Z3.

Method-4 [20]

Equivalent volume of Zn $(CH_3COO)_2{\cdot}2H_2O$ (0.5 M) and sodium hydroxide (1.5 M) were mixed to obtain a solution A. 2.5 g of PEG-6000 was dissolved in 10 ml of water to obtain solution B. The solution B was then added into solution A to obtain solution C. 50 ml of 1-octanol was added to solution C under stirring at room temperature to obtain solution D. Then solution D was transferred to Teflon lined stainless steel autoclave which was then maintained at 180 °C for 4 h under autogenous pressure. The ZnO powder was obtained after filtering, washing and drying in oven at 120 °C. The sample is designated as Z4.

Method-5

The solution of Zn $(CH_3COO)_2{\cdot}2H_2O$ (0.1 M) was prepared in 50 ml methanol under stirring. 25 ml of NaOH (0.3 M) solution, prepared in methanol, was mixed with above solution under continuous stirring to get the pH of reactants between 8 and 11, and then 4 g of sepiolite was added with vigorous stirring. It was then transferred into a Teflon lined sealed stainless steel autoclave and maintained at 150 °C for 12 h under autogenous pressure. Subsequently, it was allowed to cool naturally to room temperature. After the reaction was complete, the resulting white solid product was washed with methanol, filtered and then dried in a laboratory oven at 100 °C. The sample is designated as Z5.

Method-6

0.1 M solution of $Zn(CH_3COO)_2{\cdot}2H_2O$ in 50 ml methanol was prepared. To this solution, 0.5 mol of MgO was added. 25 ml of NaOH (0.3 M) solution, prepared in methanol, was mixed with above solution under continuous stirring to get the pH of reactants between 8 and 11. After that it was transferred into Teflon lined sealed stainless steel autoclave and maintained at 150 °C for 12 h under autogenous pressure. It was then allowed to cool naturally to room temperature. After the completion of the reaction, resulting white solid products were washed with methanol, filtered and dried in a laboratory oven at 100 °C. The sample is designated as Z6.

Characterization of zinc oxide particles

X-ray diffraction (XRD)

X-ray diffraction analysis was done using X-ray diffractometer, Rigaku "Mini flex" model in the range of 10 to 80° (=2θ). The zinc oxide powder was deposited on the sample holder uniformly.

Brunauer Emmet Teller (BET) surface area measurement

BET surface area determination was done from N_2 adsorption data measured at 77.4 K using micromeritics-ASAP-2020 instrument. The samples were activated at 200 °C for 20 min under vacuum (10 mmHg) prior to measurements. Five point BET surface area and total pore volume were measured. The average of five reading is reported here.

Transmission electron microscopy (TEM)

Morphology of different ZnO samples was investigated by transmission electron microscopy (TEM) (JEOL 2010) having LaB_6 filament, operating at an accelerating voltage of 200 kV. ZnO powder samples were dispersed by ultrasonication in acetone for 30 min. A copper grid was immersed in and taken out of the suspension and dried at room temperature. Image analysis of the microphotographs was performed using UTHSCSA Image Tool for Windows Version 3.00. It was used to determine the particle size distribution.

Differential scanning calorimetry (DSC)

Cure-studies were done using differential scanning calorimetric analysis. It was carried out using modulated DSC (DSC 2910, TA Instruments, USA). The samples were heated from ambient temperature to 250 °C (at 5 °C min^{-1} heating rate) in air. 5 mg of each sample was taken for the measurement. The error limit in the 'weighing measurements' was within ±5%.

Elemental analysis

Elemental analysis was done using a Perkin Elmer (Model: Optima 4300 DV) inductively coupled plasma-optical emission spectroscopy (ICP-OES).

Scanning electron microscopy (SEM)

SEM samples were fractured in liquid nitrogen immersion and mounted with carbon tape wrapping. The images were studied with a Nova NanoSEM 650 instrument, FEI, USA, operating at 1 and 10 kV for the micro and synthesized nano-ZnO samples, respectively.

Preparation of rubber composites

Compounding and vulcanization

ZnO was mixed with rubber by melt mixing method using Brabender Plasticorder (PL2000, Germany) internal mixer (volume 50 cm^3) for 3 min at 80 °C and 60 rpm. The formulation is given in Table 1. It was chosen as a typical tire-tread formulation. Amount of ZnO used (0.5, 1.5 and 3 phr) was lower than that used (5 phr) in the conventional formulations. The sample was then passed through a cold two roll open mixing mill at a friction ratio 1:1.2. The curing studies were followed with an Oscillating Disc Rheometer (ODR-2000, FLEXSYS) at 145 °C temperature and oscillating arc of 3° for 1 h. The samples were then compression molded at 145 °C at optimum cure time.

Physico-mechanical properties of rubber composites

Tensile test

Tensile test of the sample was carried out according to ASTM D412-98a on dumbbell shaped specimens using Instron 3367 universal testing machine at ambient temperature at a crosshead speed of 500 mm min^{-1}. Average of five samples is reported here.

Hardness

Hardness of each composition was obtained using Shore A Durometer tester as per ASTM D 2240-97.

Volume fraction of rubber (V_r) and crosslink density

The cured samples were immersed in toluene for 72 h at 25 °C temperature. The volume fraction of rubber in the swollen gel, at equilibrium swelling, was calculated using Eq. (1):

$$V_{\mathrm{r}} = \frac{(\mathrm{D} - \mathrm{FT})\rho_r^{-1}}{(\mathrm{D} - \mathrm{FT})\rho_{\mathrm{r}}^{-1} + A_0\rho_{\mathrm{s}}^{-1}}, \quad (1)$$

where D Deswollen weight, F weight fraction of the insoluble component, T initial weight of the test specimen, ρ_{r} density of rubber, 0.89 g cm^{-3}, ρ_{s} density of solvent, 0.86 g cm^{-3}, A_0 amount of solvent absorbed.

Further, the crosslink density, $\frac{1}{2M_{\mathrm{C}}}$, in mol g^{-1} of rubber hydrocarbon was calculated using the Flory–Rehner Eq. (2):

$$-\left[\ln(1 - V_{\mathrm{r}}) + V_{\mathrm{r}} + \chi V_{\mathrm{r}}^2\right] = \frac{\rho_{\mathrm{r}} V\left(V_{\mathrm{r}}^{1/3} - V_{\mathrm{r}}/2\right)}{2M_{\mathrm{C}}}, \quad (2)$$

χ Flory–Huggins interaction parameter, 0.46 for BR-toluene system [25], V molar volume of swelling solvent, toluene, M_{C} number average molecular weight of the chain between two crosslinks.

Table 1 Formulation and designation of different rubber compounds

Ingredients	SBWZ	SBSZ	SBZ1	SBZ2	SBZ3	SBZ4	SBZ5	SBZ6	0.5SBZ4	1.5SBZ4	0.5SBZ5	1.5SBZ5	SBSZF	SBZ4F	SBZ5F
SBR	70	70	70	70	70	70	70	70	70	70	70	70	70	70	70
BR	30	30	30	30	30	30	30	30	30	30	30	30	30	30	30
Sulfur	1.3	1.3	1.3	1.3	1.3	1.3	1.3	1.3	1.3	1.3	1.3	1.3	1.3	1.3	1.3
CBS	1.3	1.3	1.3	1.3	1.3	1.3	1.3	1.3	1.3	1.3	1.3	1.3	1.3	1.3	1.3
ZnO	0	3	3	3	3	3	3	3	0.5	1.5	0.5	1.5	3	3	3
6PPD	2	2	2	2	2	2	2	2	2	2	2	2	2	2	2
Wax	1	1	1	1	1	1	1	1	1	1	1	1	1	1	1
Stearic acid	0	2	2	2	2	2	2	2	2	2	2	2	2	2	2
Carbon black	0	0	0	0	0	0	0	0	0	0	0	0	60	60	60
Naphthenic oil	0	0	0	0	0	0	0	0	0	0	0	0	8	8	8

Formulation of compounds is expressed in phr (parts per hundred rubber)

Results and discussion

Characterization of nano-ZnO

XRD

Figure 1 shows the XRD patterns of different zinc oxide (ZnO) samples. The sharp intense peaks, confirming the good crystalline nature of synthesized ZnO, correspond to (100), (002), (101), (102), (110), (103), (200), (112), (201) and (004) planes. All of the indexed peaks in the obtained diffractograms match with that of the bulk ZnO (JCPDS card # 79-0207) which confirm that the synthesized samples are of wurtzite hexagonal structure [26]. Any other peak related to impurities was not detected in the diffractogram within the detection limit of the XRD. Absence of any extra peak in the diffractograms of final products indicates the purity of the products. In Z5, additional peaks can be observed, other than the earlier mentioned peaks for ZnO. These are for (060), (131) [at 20°], (260) [at 24°] and (080, 331) planes [at 27°, 28°] of sepiolite clay [27]. It proves that ZnO particles are formed on sepiolite without distorting the crystal structure of either material.

The average crystal size was calculated by Scherrer Eq. 28]:

$$L = \frac{K\lambda}{\beta \cos\theta}, \tag{3}$$

where, β is the full-width at half maximum (FWHM) of the peak corresponding to (100) plane, K is a constant (0.89), λ is the incident wavelength of CuK_α radiation ($\lambda = 0.154$ nm), L is the crystallite size, and θ is the diffraction angle at a certain crystal plane.

The average crystallite size of Z1, Z2, Z3, Z4, Z5 and Z6 was calculated using Eq. (3) and was found to be 23, 20, 18, 27, 27 and 16 nm, respectively. It should be noted that crystallite size is assumed to be the size of a coherently diffracting domain. It is not necessarily the same as particle size [28].

BET surface area

BET surface area of different prepared nano-ZnO is reported in Table 2. Surface area and pore volume both increase in the synthesized ZnO samples compared to the reference one. Highest surface area and pore volume can be observed in the case of Z5. This could be due to dispersion of ZnO particles on the fibrous sepiolite template surface. For the same sample, smallest particle size was also observed through TEM (Fig. 2e). So the surface area results corroborate well with the microscopic study. The sample Z4 shows minimum surface area among the synthesized samples, as it is coated with PEG. The organic coating of PEG resists the nitrogen to be absorbed on the surface of ZnO particles.

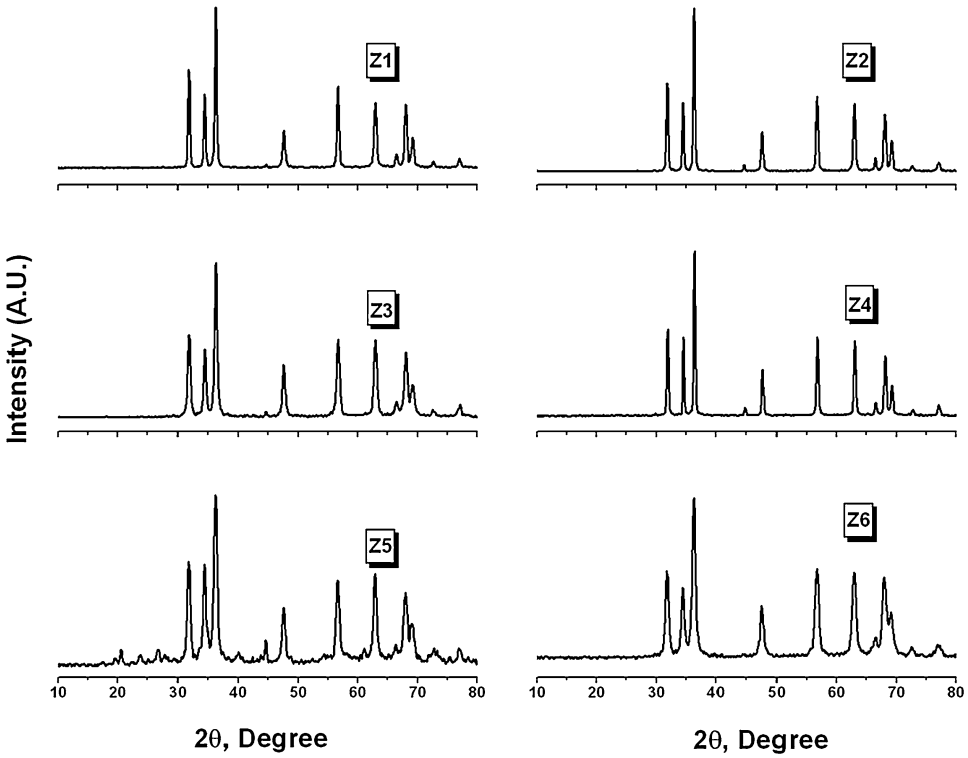

Fig. 1 X-ray diffractogram of the different zinc oxide samples

Table 2 Crystallite size of different zinc oxide samples

Sample	FWHM of (100) plane (degree)	Average crystallite size (nm)
Z1	0.3444	23
Z2	0.3936	20
Z3	0.4428	18
Z4	0.2952	27
Z5	0.2952	27
Z6	0.4920	16

TEM

Figure 2a–f portrays TEM photo-micrographs of different zinc oxide (ZnO) samples. TEM image exhibits the morphology of synthesized particles to be in nano region. Samples Z1, Z2, Z3, Z5 and Z6 show hexagonal structure. The particle size distribution curves for these samples are shown in Fig. 3. It shows that for Z1, maximum particles are in the range of 26–50 nm; for Z2, it is also in the range of 26–50 nm and for Z3, it is in the range of 15–28 nm. The sample Z4 evinces rod-like structures grown on PEG-sheets. The average rod diameter is ~50 nm. These nano-rods are of 100–200 nm in length. Z5 exhibits an interesting morphology; it consists of smallest ZnO particles. Figure 2e infers that ZnO nanoparticles are grown on long bundles of sepiolite nanofibers. The ZnO particles are very small in size; most of the particles are in 7–12 nm range. Sample Z6 has maximum particles in the range of 10–18 nm.

Application of synthesized nano-ZnO

Cure properties

The effect of synthesized nano-ZnO as cure activator has been studied on SBR/BR blend. A representative rheographic profile of SBR/BR blends at 145 °C is shown in Fig. 4 and cure time is tabulated in Table 3. In the absence of ZnO, the curing is extremely slow in the sample SBWZ and modulus is also lowest. The optimum cure time is faster with synthesized nano-ZnO samples by complex formation with acceleration compared to the reference one. ZnO helps in producing vulcanization precursor, hence faster curing can be observed in the presence of ZnO [29]. Due to decrease in particle size of ZnO, the area of contact increases which helps to react better with accelerator. This leads to the generation of vulcanization precursor quicker. It results in a faster curing rate and lower cure time. Fastest curing can be seen with the use of organo-coated ZnO, Z4, followed by Z5. Due to the presence of long-chain organic PEG molecules, it has more compatibility with elastomeric matrix leading to better dispersion. The curing reaction is not affected and slowed down in the presence of Z4 at lower dose, i.e., 0.5 and 1.5 phr. It indicates that dispersion of ZnO plays a major role in efficient vulcanization, rather

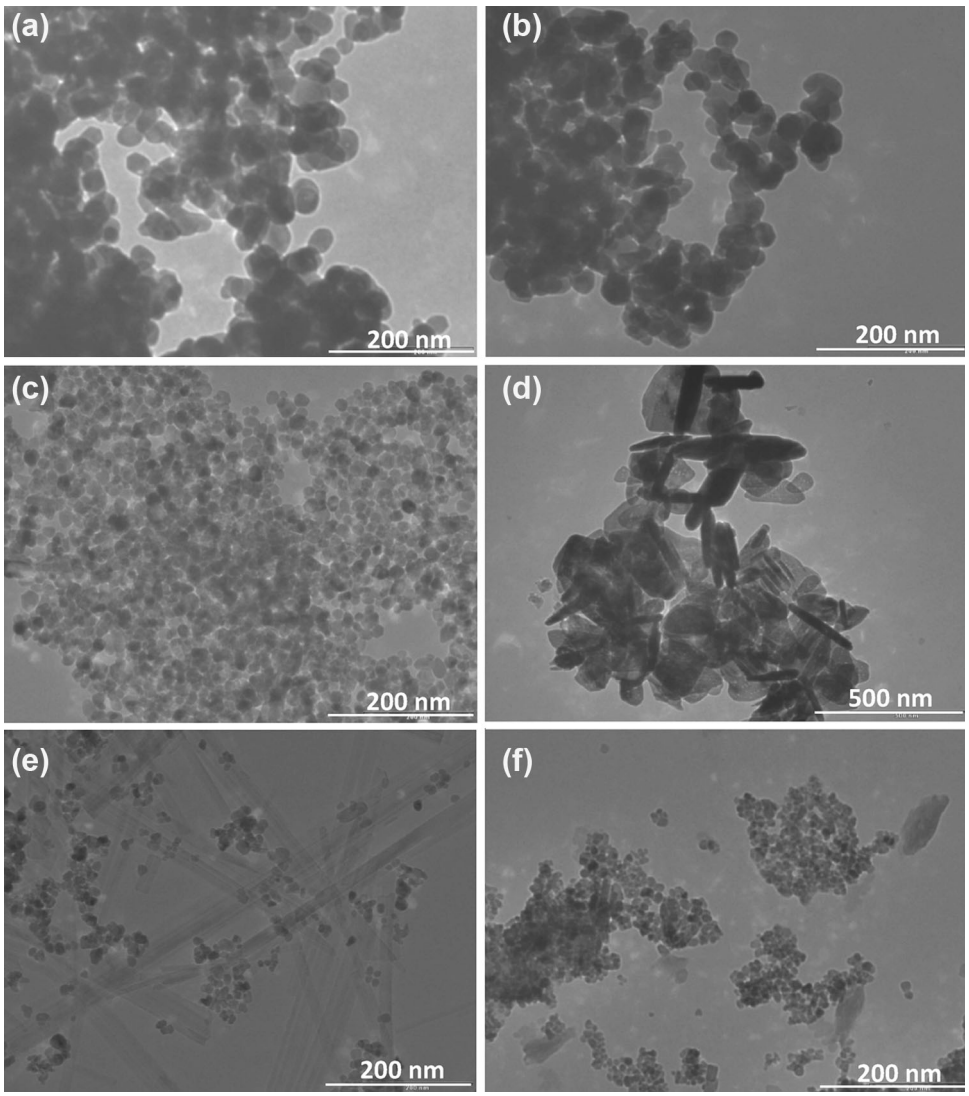

Fig. 2 TEM image of the sample **a** Z1, **b** Z2, **c** Z3, **d** Z4, **e** Z5 and **f** Z6

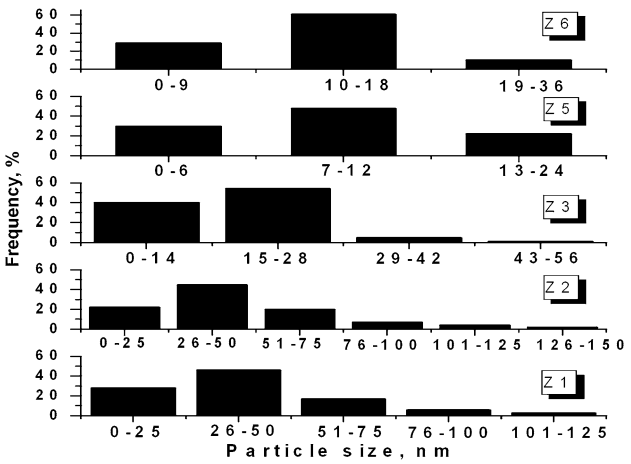

Fig. 3 Particle size distribution curves of different ZnO samples

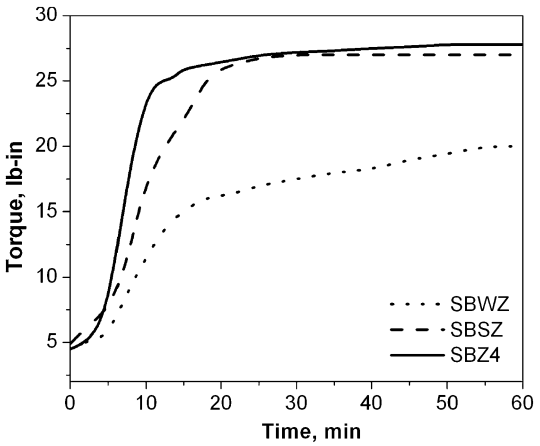

Fig. 4 Representative rheographic profiles of SBR/BR blends containing different ZnO samples

than higher loading of ZnO. The difference in minimum (M_L) and maximum (M_H) torque value, [$\Delta S = (M_H - M_L)$] has increased in SBR/BR blend with the use of synthesized nano-ZnO compared to that of reference ZnO based sample. Increased ΔS indicates resistance to polymer chain mobility [30]. Due to the formation of increased crosslinks, chain mobility is restricted which will lead to higher crosslink density. In the case of Z5, the template, sepiolite which is fibrous clay with high aspect ratio, can help in better distribution of ZnO particles. As mentioned earlier, the area of contact increases in such case and helps in generation of vulcanizing precursors faster. These nano-ZnO samples impart better co-curing of both the rubbers in SBR/BR blend.

Table 3 BET value of different nano-ZnO samples

Sample	Surface area ($m^2\ g^{-1}$)	Pore volume ($cm^3\ g^{-1}$)
Reference ZnO, SZ	5	0.025
Z1	18	0.123
Z2	11	0.084
Z3	39	0.110
Z4	5	0.039
Z5	104	0.230
Z6	55	0.110

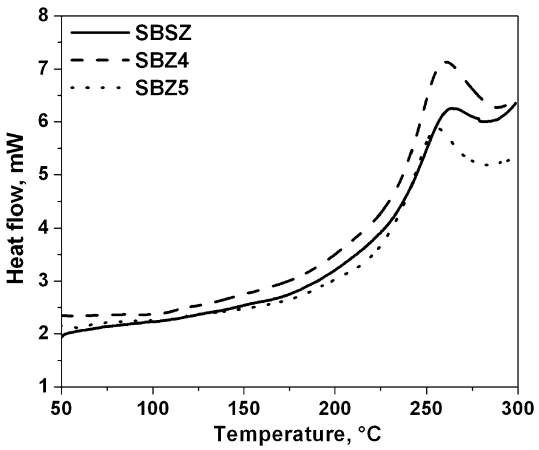

Fig. 5 *DSC curves* of different ZnO containing SBR/BR compounds depicting dynamic curing

The presence of very little amount of magnesium in Z6 (Zn:Mg 90:1, as revealed from ICP-OES analysis) has visible impact on cure properties. It increases the optimum cure time but at the same time it also increases ΔS values. It produces maximum number of crosslinks but at a slower rate.

Most encouraging effect of synthesized nano-ZnO on curing can be observed in the presence of filler. Optimum cure time is lowered by 7–10 min in the case of synthesized nano-ZnO containing compounds compared to the reference ZnO based compound (which even contains higher dose of ZnO). Thus, ZnO nanoparticles can help in the reduction of the production cycle and also in minimizing the Zn-pollution due to lower dose.

Cure behavior in dynamic condition is shown in the representative plots (Fig. 5). The results differ slightly from static curing, though Z4 shows most efficient crosslinking activities ($\Delta H = 123.70\ Jg^{-1}$) in dynamic curing, too (Table 4).

Physico-mechanical properties of different rubber composites

The nano-ZnO particles may also act as nano-fillers. Physico-mechanical properties of different rubber composites

Table 4 Cure properties of different elastomeric compounds

Sample	Cure time, t_{90} (min)	M_H (lb-in)	M_L (lb-in)	$M_H - M_L$ (lb-in)
SBWZ	38.2 (0.08)[a]	20.28 (0.07)	3.97 (0.14)	16.31
SBSZ	18.5 (0.10)	27.01 (0.10)	4.87 (0.13)	22.14
SBZ1	17.0 (0.09)	27.43 (0.15)	3.62 (0.09)	23.81
SBZ2	16.9 (0.07)	28.03 (0.20)	3.72 (0.10)	24.31
SBZ3	16.4 (0.12)	28.35 (0.04)	4.12 (0.08)	24.23
SBZ4	12.9 (0.07)	27.85 (0.13)	4.05 (0.02)	23.80
SBZ5	13.0 (0.11)	28.74 (0.09)	4.48 (0.04)	24.46
SBZ6	19.2 (0.08)	30.16 (0.07)	5.03 (0.05)	25.13
0.5SBZ4	12.2 (0.07)	27.93 (0.13)	4.42 (0.04)	23.51
1.5SBZ4	12.5 (0.10)	27.87 (0.14)	4.43 (0.03)	23.44
SBSZF	25.3 (0.07)	35.83 (0.21)	6.95 (0.12)	28.88
SBZ4F	15.6 (0.09)	43.76 (0.23)	8.01 (0.14)	35.75
SBZ5F	18.0 (0.04)	39.88 (0.24)	7.45 (0.11)	32.43

[a] Values in parentheses are standard deviations

are reported in Table 5. Z2, Z3, Z4 and Z5 containing SBR/BR blend based nanocomposites show better tensile strength and hardness compared to the reference one. The sample containing organo-coated ZnO (Z4) displays highest tensile strength. This is ascribed to the better compatibility and in turn better dispersion of Z4 in the rubber matrix. This leads to better curing as observed in the previous experiments and higher value of volume fraction of rubber (V_r) as well as crosslink density. Z4 imparts highest reinforcement. From these results it can be concluded that dispersion of nanoparticles plays the major role in enhancement of properties.

Though lower filler loading maintains the cure properties unaltered (as observed in 0.5SBZ4 and 1.5SBZ4) but it does not provide the same amount of reinforcement as 3 phr loading. Tensile strength, 100% modulus and hardness decrease with decreasing ZnO loading.

Nano-ZnO containing compounds show slightly better properties than those of reference ZnO based compound. Z5 based compound exhibits highest overall properties. This may be due to some synergistic effect between nanofiller, sepiolite and conventional filler, carbon black [31]. The similar kind of effect has also been studied in our previous study using mesoporous silica as reinforcing filler in the poly butadiene rubber matrix in the presence of nanoclays, silica and carbon black [32].

Table 5 Dynamic cure properties of different elastomeric compounds

Sample	T_{max} (°C)	ΔH (J g^{-1})
SBSZ	261	63.66
SBZ2	261	88.39
SBZ3	262	81.06
SBZ4	258	123.70
SBZ5	254	86.58
SBZ6	260	92.92

Morphology

The topographical images of SEM shown in Fig. 6 of different SBR/BR blend either having synthesized nano-ZnO or standard rubber grade-ZnO is studied to evaluate the extent of dispersion of ZnO within the rubber blend. The black phase implies the rubber matrix, whereas the white dot is the reflection of ZnO particles. In SEM images of SBSZ (Fig. 6a), some agglomeration of ZnO nanoparticles in the form of white dot can be seen. Figure 6b indicates that uniform dispersion of nano-ZnO occurs throughout the entire blend in comparison to standard rubber grade-ZnO (Fig. 5a). In case of SBZ4 (Fig. 6c), the rod-like structure as observed in TEM photo-micrographs (Fig. 2d) can also be seen. However, in the image of sepiolite based synthesized nano-ZnO (Fig. 5d), the homogenous distribution of ZnO with minimum particle

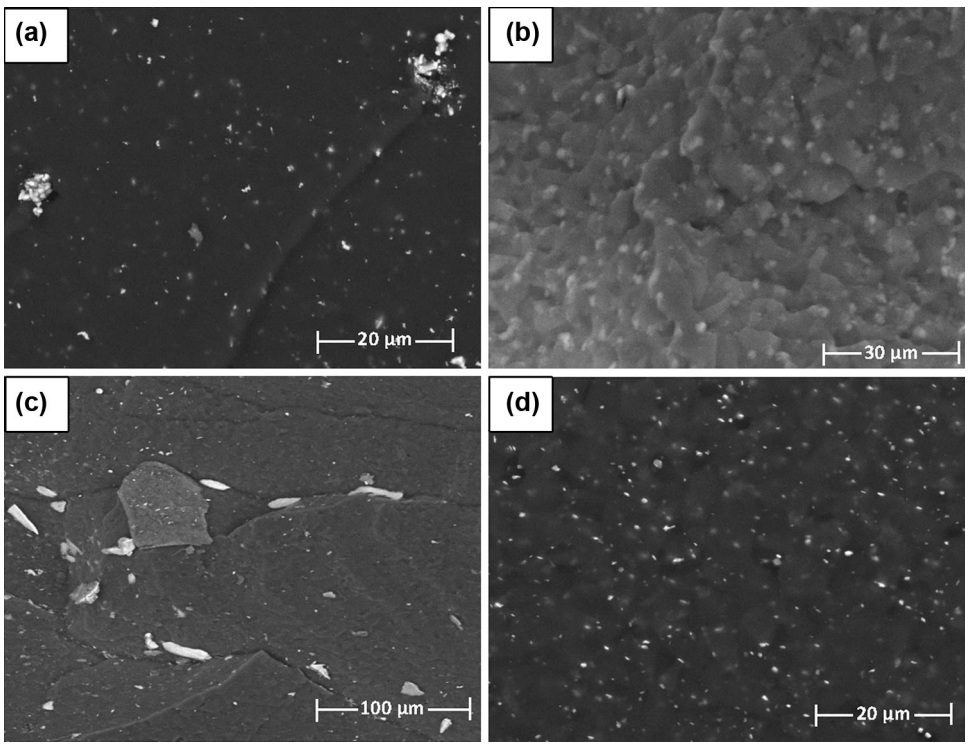

Fig. 6 SEM images of **a** SBSZ, **b** SBZ3, **c** SBZ4 and **d** SBZ5

Table 6 Physico-mechanical properties of different rubber composites

Sample	Tensile strength (MPa)	Modulus at 100% elongation (MPa)	Elongation at break (%)	Hardness (shore A)	V_r	Crosslink density $\times 10^{-5}$ mol cm^{-3}
SBWZ	1.73 (0.02)[a]	0.70 (0.02)	445 (10)	37 (0.3)	0.112 (0.003)	2.50 (0.01)
SBSZ	1.89 (0.02)	0.84 (0.03)	310 (12)	41 (0.2)	0.165 (0.002)	6.31 (0.02)
SBZ1	1.82 (0.03)	0.73 (0.03)	320 (15)	43 (0.3)	0.164 (0.002)	6.22 (0.03)
SBZ2	2.12 (0.03)	0.78 (0.04)	335 (18)	43 (0.4)	0.168 (0.003)	6.60 (0.01)
SBZ3	2.07 (0.04)	1.09 (0.03)	265 (22)	45 (0.3)	0.164 (0.004)	6.22 (0.01)
SBZ4	2.54 (0.01)	1.05 (0.02)	295 (14)	44 (0.4)	0.171 (0.002)	6.90 (0.02)
SBZ5	2.05 (0.05)	1.07 (0.02)	250 (18)	45 (0.2)	0.167 (0.002)	6.50 (0.03)
SBZ6	1.90 (0.03)	0.90 (0.03)	280 (12)	46 (0.1)	0.169 (0.003)	6.70 (0.04)
0.5SBZ4	1.61 (0.02)	0.72 (0.02)	335 (10)	37 (0.3)	0.165 (0.002)	6.31 (0.02)
1.5SBZ4	2.15 (0.01)	0.94 (0.03)	290 (17)	41 (0.2)	0.169 (0.004)	6.70 (0.01)
SBSZF	14.30 (0.5)	1.62 (0.02)	560 (09)	61 (0.1)	0.187 (0.005)	8.65 (0.04)
SBZ4F	14.84 (0.2)	1.67 (0.01)	565 (08)	63 (0.2)	0.191 (0.005)	9.13 (0.03)
SBZ5F	15.24 (0.3)	1.82 (0.01)	645 (10)	63 (0.3)	0.190 (0.007)	9.01 (0.02)

[a] Values in parentheses are standard deviations

size is observed (as seen in TEM images too) (Fig. 2e). As a result, the improvement of mechanical properties of the SBR/BR blend can be noticed (Table 5). From the SEM images, it can be distinguished that the distribution of ZnO in the SBR/BR blend is comparatively better for nano-ZnO which in turn is reflected in mechanical properties (Table 6).

Conclusions

Six different nano-ZnO samples were synthesized by both high temperature calcination and low-temperature hydrolysis methods. All the samples had wurtzite structure and average particle size in the 'nm' range. ZnO, grown on sepiolite nanofiber, showed smallest particle size as well as highest surface area. PEG-coated ZnO nanoparticles were rod-like in structure. Effect of these nano-ZnO samples on cure properties of SBR/BR blends was studied by both static and dynamic curing methods. PEG-coated nano-ZnO sample exhibited maximum positive impact on cure properties. For PEG-coated ZnO, cure properties remained unaltered even at lower loadings (0.5 and 1.5 phr) of ZnO. From the observed results, it can be concluded that the cure properties are governed primarily by dispersion of cure-activator rather than its concentration and morphology. Nano-ZnO can act as nanofiller also. The sample containing organo-coated ZnO (Z4) displays highest tensile strength due to better compatibility and in turn better dispersion of Z4 in the rubber matrix. Dosing (of nano-ZnO) lower than 3 phr could not impart any reinforcement. Topographical images of SEM study indicates more uniform dispersion of synthesized nano-ZnO over standard rubber grade-ZnO within rubber blend and this fact account for better mechanical properties. Nano-ZnO imparted faster curing even in the presence of conventional filler, carbon black compared with reference ZnO. Thus, the use of ZnO nanoparticles can provide faster curing, better reinforcement at lower dosing compared to standard ZnO, which can lead to shorter production cycles and less zinc pollution.

Acknowledgements The authors are highly thankful to Ms. Hetal Patel and Mr. Chirag S. Shah for their kind cooperation. Authors are grateful to Reliance Industries Ltd. for its consent to publish this work. Authors are also thankful to colleagues from catalyst, analytical and elastomer groups of RTG-VMD for their support.

References

1. Frohlich J, Niedermeier W, Luginsland HD (2005) The effect of filler–filler and filler–elastomer interaction on rubber reinforcement. Compos A 36:449–460
2. Schuater RH (2001) The challenge a head-new polymer filler systems. Rubber World 224:24–28
3. Morton M (1959) Introduction to rubber technology. Reinhold Publishing Corporation, New York
4. Councell TB, Duckenfield KU, Landa ER, Callender E (2004) Tire-wear particles as a source of zinc to the environment. Environ Sci Technol 38:4206–4214
5. Smolders E, Degryse F (2002) Fate and effect of zinc from tire debris in soil. Environ Sci Technol 36:3706–3710

6. Heideman G, Noordermeer JWM, Datta RN, Baarle BV (2005) Effect of metal oxides as activator for sulphur vulcanisation in various rubbers. Kautschuk Gummi Kunststoffe 58:30–42
7. Basu D, Das A, Stockelhuber KW, Wagenknecht U, Heinrich G (2014) Advances in layered double hydroxide (LDH)-based elastomer composites. Prog Polym Sci 39:594–626
8. Sahoo S, Maiti M, Ganguly A, George JJ, Bhowmick AK (2007) Effect of zinc oxide nanoparticles as cure activator on the properties of natural rubber and nitrile rubber. J Appl Polym Sci 105:2407–2415
9. Sahoo S, Bhowmick AK (2007) Influence of ZnO nanoparticles on the cure characteristics and mechanical properties of carboxylated nitrile rubber. J Appl Polym Sci 106:3077–3083
10. Sahoo S, Kar S, Ganguly A, Maiti M, Bhowmick AK (2008) Synthetic zinc oxide nanoparticles as curing agent for polychloroprene. Polym Polym Compos 16:193–198
11. Sabura Begum PM, Yusuff KKM, Joseph R (2008) Preparation and use of nano zinc oxide in neoprene rubber. Int J Polym Mater 57:1083–1094
12. Sabura Begum PM, Joseph R, Yusuff KKM (2008) Preparation of nano zinc oxide, its characterization and use in natural rubber. Prog Rubber Plast Recycl 24:141–148
13. Przybyszewska M, Zaborski M (2009) New coagents in crosslinking of hydrogenated butadiene-acrylonitrile elastomer based on nanostructured zinc oxide. Compos Interfaces 16:131–141
14. Przybyszewska M, Zaborski M (2010) Effect of ionic liquids and surfactants on zinc oxide nanoparticle activity in crosslinking of acrylonitrile butadiene elastomer. J Appl Polym Sci 116:155–164
15. Przybyszewska M, Zaborski M (2009) The effect of zinc oxide nanoparticle morphology on activity in crosslinking of carboxylated nitrile elastomer. Express Polym Lett 3:542–552
16. Guzman M, Reyes G, Agullo N, Borros S (2011) Synthesis of Zn/Mg oxide nanoparticles and its influence on sulfur vulcanization. J Appl Polym Sci 119:2048–2057
17. Heideman G, Datta RN, Noordermeer JWM, Van Baarle B (2005) Influence of zinc oxide during different stages of sulfur vulcanization. Elucidated by model compound studies. J Appl Polym Sci 95:1388–1404
18. Kim I, Kim W, Lee D, Kim W, Bae J (2010) Effect of nano zinc oxide on the cure characteristics and mechanical properties of the silica-filled natural rubber/butadiene rubber compounds. J Appl Polym Sci 117:1535–1543
19. Jincheng W, Yuehui CJ (2006) Application of nano-zinc oxide master batch in polybutadiene styrene rubber system. J Appl Polym Sci 101:922–930
20. Maiti M, Vaghasia A, Jasra RV (2012) Low-temperature synthesis of nano-to-submicron size organo-zinc oxide and its effect on properties of polybutadiene rubbe. J Appl Polym Sci 124:2857–2866
21. Wang J, Chen Y (2006) Application of nano-zinc oxide master batch in polybutadiene styrene rubber system. J Appl Polym Sci 101:922–930
22. Qi JY, Wu LX, Zhuo DX (2014) Preparation and properties of BR/SBR blends using surface-modified nano zinc oxide". Adv Mater Res 910:101–104
23. Sridevi D, Rajendran KV (2009) Synthesis and optical characteristics of ZnO nanocrystals. Bull Mater Sci 32:165–168
24. Aneesh PM, Jayaraj MK (2010) Red luminescence from hydrothermally synthesized Eu-doped ZnO nanoparticles under visible excitation. Bull Mater Sci 33:227–231
25. Gundert F, Wolf BA (1989) Solvents and non-solvents for polymers. In: Brandrup J, Immergut EM (eds) Polymer handbook, 3rd edn. Wiley, New York, VII, pp 173–182
26. Bhattacharyya S, Gedanken A (2008) A template-free, sonochemical route to porous ZnO nano-disks. Microporous Mesoporous Mater 110:553–559
27. Yalcin H, Bozkaya O (1995) Sepiolite-palygorskite from the Hekimhan region clay. Clay Miner 43:705–717
28. Monshi A, Foroughi MR, Monshi MR (2012) Modified Scherrer equation to estimate more accurately nano-crystallite size using XRD. World J Nano Sci Eng 2:154–160
29. Blow CM, Hepburn C (1982) Rubber technology and manufacture. Butterworth Scientific, London
30. Shamugharaj AM, Bae JH, Lee KY, Noh WH, Lee SH, Rye SH (2007) Physical and chemical characteristics of multiwalled carbon nanotubes functionalized with aminosilane and its influence on the properties of natural rubber composites. Comp Sci Technol 67:1813–1822
31. Maiti M, Sadhu S, Bhowmick AK (2005) Effect of carbon black on properties of rubber nanocomposites. J Appl Polym Sci 96:443–451
32. Maiti M, Basak GC, Srivastava VK, Jasra RV (2016) Mesoporous silica reinforced polybutadiene rubber hybrid composite. Int J Ind Chem 7:131–141